

1 **Fast particulate nitrate formation via N₂O₅ uptake aloft in winter Beijing**

2 *Haichao Wang¹, Keding Lu^{1*}, Xiaorui Chen¹, Qindan Zhu^{1, #}, Zhijun Wu¹, Yusheng*
3 *Wu¹, Kang Sun²*

4 ¹State Key Joint Laboratory of Environmental Simulation and Pollution Control, College of
5 Environmental Sciences and Engineering, Peking University, Beijing, China

6 ²China National Environmental Monitoring Centre, Beijing, China

7 [#]Now at the Department of Chemistry, University of California, Berkeley, CA 94720, USA

8
9 *Correspondence to: *Keding Lu* (k.lu@pku.edu.cn)

10
11 **Abstract.**

12 Particulate nitrate (pNO₃⁻) is an important component of secondary aerosols in urban
13 areas. Therefore, it is critical to explore its formation mechanism to assist with the
14 planning of haze abatement strategies. Here we report vertical measurement of NO_x
15 and O₃ by in-situ instruments on a movable carriage on a tower during a winter
16 heavy-haze episode (December 18 to 20, 2016) in urban Beijing, China. Based on the
17 box model simulation at different height, we found that pNO₃⁻ formation via N₂O₅
18 heterogeneous uptake was negligible at ground level due to N₂O₅ concentration of
19 near zero controlling by high NO emission and NO concentration. In contrast, the
20 contribution from N₂O₅ uptake was large at high altitudes (e.g., > 150 m), which was
21 supported by the low total oxidant (NO₂ + O₃) level at high altitudes than that at
22 ground level. Modeling results show the specific case that the nighttime integrated
23 production of pNO₃⁻ for the high-altitude air mass above urban Beijing was estimated
24 to be 50 μg m⁻³ and enhanced the surface-layer pNO₃⁻ the next morning by 28 μg m⁻³
25 through vertical mixing. Sensitivity tests suggested that the nocturnal NO_x loss by
26 NO₃-N₂O₅ chemistry was maximized once the N₂O₅ uptake coefficient was over
27 2×10⁻³ on polluted days with S_a was 3000 μm² cm⁻³ in wintertime. The case study

28 provided a chance to highlight that pNO_3^- formation via N_2O_5 heterogeneous
29 hydrolysis may be an important source of the particulate nitrate in the urban airshed
30 during wintertime.

31

32 **1. Introduction**

33 Winter particulate matter (PM) pollution events occur frequently in China and have
34 drawn widespread and sustained attention in recent years (Guo et al., 2014; Zhang et
35 al., 2015; Huang et al., 2014; Wang G et al., 2016). PM pollution reduces visibility
36 (Lei and Wuebbles, 2013) and has harmful effects on public health (Cao et al., 2012).
37 Particulate nitrate (pNO_3^-) is an important component of secondary inorganic aerosols
38 and contributes 15% – 40% of the $\text{PM}_{2.5}$ mass concentration in China (Sun et al., 2013,
39 2015a, 2015b; Chen et al., 2015; Zheng et al., 2015; Wen et al., 2015). The main
40 atmospheric pathways of nitrate formation are (1) the reaction of OH with NO_2 and (2)
41 N_2O_5 heterogeneous hydrolysis (Seinfeld and Pandis, 2006). The reaction of OH with
42 NO_2 is a daytime pathway, as OH is very low in concentration at night, and N_2O_5
43 uptake is a nighttime pathway, as NO_3 and N_2O_5 are easily photo-labile.

44 Particulate nitrate formation via N_2O_5 heterogeneous hydrolysis in summer was
45 proved efficient by ground-based observation in North China (Wang H et al., 2017b;
46 Wang Z et al., 2017), and found comparable to or even higher than the daytime
47 formation. Several studies showed that N_2O_5 hydrolysis is responsible for nocturnal
48 pNO_3^- enhancement in summer Beijing (Pathak et al., 2009, 2011; Wang H et al.,
49 2017a). Although pNO_3^- formation via N_2O_5 uptake is significant in summertime, the
50 importance of this pathway in wintertime is not well characterized. Many differences
51 in N_2O_5 chemistry exist between winter and summer. First, as the key precursor of
52 NO_3 and N_2O_5 , O_3 has a much lower concentration in winter than in summer, owing
53 to the short daytime length and weak solar radiation. Second, colder temperature and
54 high NO_2 level favor the partitioning towards N_2O_5 . Third, longer nighttime length in
55 winter makes N_2O_5 heterogeneous hydrolysis potentially more important in pNO_3^-
56 formation. Finally, the N_2O_5 uptake coefficient, as an important parameter in N_2O_5

57 heterogeneous hydrolysis, is likely very different from that in summer. This is because
58 the properties of aerosol particles (e.g., organic compounds, particulate nitrate, liquid
59 water contents, solubility, and viscosity) and meteorological conditions (e.g.,
60 temperature and relative humidity) differ between summer and winter (Chen et al.,
61 2015; Zhang et al., 2007). These effects would result in large variations in the N_2O_5
62 uptake coefficient (Wahner et al., 1998; Mentel et al., 1999; Kane et al., 2001;
63 Hallquist et al., 2003; Thornton et al., 2003; Bertram and Thornton, 2009; Tang et al.,
64 2012; Wagner et al., 2013; Grzinic et al., 2015). Several parameterization methods did
65 not have good performance in predicting N_2O_5 uptake coefficient accurately (Chang et
66 al., 2011; Chang et al., 2016).

67 In addition to the seasonal differences in pNO_3^- formation via N_2O_5 uptake,
68 modeling and field studies showed high levels of NO_3 and N_2O_5 at high altitudes
69 within the nocturnal boundary layer (NBL), owing to the stratification of surface NO
70 and volatile organic compounds (VOCs) emissions, which lead to gradients in the loss
71 rates for these compounds as a function of altitude (e.g., Brown et al., 2007; Geyer
72 and Stutz, 2004; Stutz et al., 2004). The pNO_3^- formation via N_2O_5 uptake contributes
73 to the gradients in the compounds percentage and size distribution of the particle
74 (Ferrero et al., 2010; 2012). On nights when NO_3 can't accumulate in the surface
75 layer owing to high NO emissions, N_2O_5 uptake can still be active aloft without NO
76 titration. The N_2O_5 uptake aloft leads to elevated pNO_3^- formation in the upper layer
77 as well as effective NO_x removal (Watson et al., 2002; S. G. Brown et al., 2006;
78 Lurmann et al., 2006; Pusede et al., 2016; Baasandorj et al., 2017). Field observations
79 at high altitude sites of Kleiner Feldberg, Germany (Crowley et al., 2010a); the
80 London British Telecommunications tower, UK (Benton et al., 2010); and Boulder,
81 CO, USA (Wagner et al., 2013) showed the elevated N_2O_5 concentrations aloft. Model
82 studies showed that pNO_3^- varied at different heights and stressed the importance of
83 the heterogeneous formation mechanism (Kim et al., 2014; Ying, 2011; Su et al.,
84 2017). The mass fraction and concentration of pNO_3^- in Beijing was reported higher
85 aloft (260 m) than at the ground level in Beijing (Chan et al., 2005; Sun et al., 2015b),
86 which was explained by favorable gas-particle partitioning aloft under lower

87 temperature conditions. Overall, the active nighttime chemistry in the upper level
88 plays an important role in surface PM pollution through mixing and dispersing within
89 the planet boundary layer (PBL) (Prabhakar et al., 2017), the pollution was even
90 worse in valley terrain regions coupled with adverse meteorological processes
91 (Baasandorj et al., 2017; Green et al., 2015).

92 To explore the possible sources of pNO_3^- and the dependence of its formation on
93 altitude in wintertime in Beijing, we conducted vertical profile measurements of NO ,
94 NO_2 , and O_3 with a moving cabin at a tower platform in combination with
95 simultaneous ground measurements of more comprehensive parameters in urban
96 Beijing. A box model was used to investigate the reaction rate of N_2O_5 heterogeneous
97 hydrolysis and its impact on pNO_3^- formation at different altitudes during a heavy
98 haze episode over urban Beijing. Additionally, the dependence of NO_x removal and
99 pNO_3^- formation on the N_2O_5 uptake coefficient was probed.

100

101 **2. Methods**

102 **2.1 Field measurement**

103 Ground measurements (15 m above the ground) were carried out on the campus of
104 Peking University (PKU; $39^\circ59'21''\text{N}$, $116^\circ18'25''\text{E}$) in Beijing, China. The vertical
105 measurements were conducted at the Institute of Atmospheric Physics (IAP), Chinese
106 Academy of Sciences ($39^\circ58'28''\text{N}$, $116^\circ22'16''\text{E}$). The IAP site is within 4 km of the
107 PKU site. The locations of the PKU and IAP sites are shown in Fig. 1. At the PKU
108 site, dry-state mass concentration of $\text{PM}_{2.5}$ was measured using a TEOM 1400A
109 analyzer. NO_x was measured via a chemiluminescence analyzer (Thermo Scientific,
110 TE-42i-TR), and O_3 was measured with a UV photometric O_3 analyzer (Thermo
111 Scientific, TE-49i). Dry-state particle number and size distribution (PNSD) was
112 measured from 0.01 to 0.7 μm with a Scanning Mobility Particle Sizer (SMPS; TSI
113 Inc. 3010). The instrumental parameters are summarized in Table S1. The data were
114 collected from December 16 to 22, 2016. Additionally, relative humidity (RH),
115 temperature (T), and wind direction and speed data were available during the

116 measurement period.

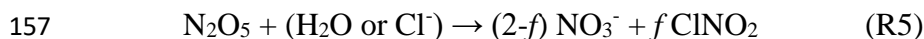
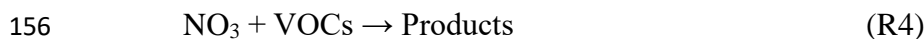
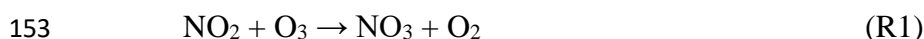
117 Vertical profile measurements were conducted from December 18 to 20, 2016, from
118 the tower-based platform (maximum height: 325 m) on the IAP campus. The NO_x and
119 O₃ instruments were installed aboard a movable cabin on the tower. NO_x and O₃ were
120 measured with two low-power, lightweight instruments (Model 405 nm and Model
121 106-L, 2B Technologies, USA). The Model 405 nm instrument measures NO₂ directly
122 based on the absorbance at 405 nm, and NO is measured by adding excess O₃
123 (conversion efficiency ~100%). The limit of detection of both NO and NO₂ is 1 part
124 per billion volume (ppbv), with an accuracy of 2 ppbv or 2% of the reading, and the
125 time resolution is 10 s (Birks et al., 2018). The Model 106-L instrument measures O₃
126 based on the absorbance at 254 nm, with a precision of 1 ppbv, or 2% of the reading,
127 and a limit of detection of 3 ppbv. NO_x calibration was performed in the lab using a
128 gas calibrator (TE-146i, Thermo Electron, USA) associated with a NO standard (9.8
129 ppmv). The O₃ calibration was done with an O₃ calibrator (TE 49i-PS), which was
130 traceable to NIST (National Institute of Standards and Technology) standards annually.
131 Before the campaign, the NO_x monitor was compared with a Cavity Attenuated Phase
132 Shift (CAPS) Particle Light Extinction Monitor, and the O₃ monitor was compared to
133 a commercial O₃ analyzer (TE-49i, Thermo Electron, USA). Good agreement was
134 found between the portable instruments and the conventional monitors. Height
135 information was retrieved via the observed atmospheric pressure measured by the
136 Model 405 nm instrument. The cabin ascended and descended at a rate of 10 m min⁻¹,
137 with a height limit of 260 m during the daytime and 240 m at night. The cabin stopped
138 after reaching the peak, and parameters were measured continually during the last 10
139 min of each cycle. One vertical cycle lasted for approximately 1 h. We measured two
140 cycles per day, one in the morning and the other in the evening. Six cycles were
141 measured in total during the campaign.

142

143 **2.2 Box model simulation**

144 A simple chemical mechanism (see R1–R5) was used in a box model to simulate the

145 nighttime NO_3 and N_2O_5 chemistry under NO free-air-mass conditions. Physical
 146 mixing, dilution, deposition, or interruption during the transport of the air mass was
 147 not considered in the base case, the physical influence to the model result will be
 148 discussed in Sect. 3.4. Here, f represents the ClNO_2 yield from N_2O_5 uptake.
 149 Homogeneous hydrolysis of N_2O_5 and NO_3 heterogeneous uptake reaction were
 150 neglected in this analysis because of the low level of absolute humidity and the
 151 extremely low NO_3 concentration during wintertime (Brown and Stutz, 2012). The
 152 corresponding rate constants of R1–R3 are those reported by Sander et al. (2011).



158 Following the work of Wagner et al. (2013), the box model can be solved using six
 159 equations (Eqs. 1–6). In the framework, O_3 is only lost via the reaction of $\text{NO}_2 + \text{O}_3$
 160 and the change in the O_3 concentration can be expressed as Eq. 1. Eq. 2 can express
 161 the losses of NO_2 . The $s(t)$ is between 0 and 1 and expressed as Eq. 5, the physical
 162 meaning of $s(t)$ is the ratio of NO_3 production which goes through N_2O_5 (either as
 163 N_2O_5 or lost through uptake) to the total NO_3 production (Wagner et al., 2013). The
 164 $s(t)$ favors 0 when direct loss of NO_3 dominates and favors 1 when N_2O_5 uptake
 165 dominates NO_3 loss. The model calculation has two steps. The first step is calculate
 166 the mixing ratio of NO_2 and O_3 at time zero (herein designated as sunset). According
 167 to Eqs. 1 and 2, the initial NO_2 ($t=0$) and O_3 ($t=0$) concentrations can then be
 168 integrated backward in time starting with the measured concentrations of NO_2 and O_3
 169 at each height. During the pollution period in winter in Beijing ($\text{NO}_2 = 45$ ppbv,
 170 Temperature = 273 K, $S_a = 3000 \mu\text{m}^2 \text{cm}^{-3}$), the ratio of N_2O_5 to NO_3 is large enough,
 171 i.e., 450. The pseudo-first-order loss rate of N_2O_5 heterogeneous uptake will be 1×10^{-3}
 172 s^{-1} , with a N_2O_5 uptake coefficient of 5×10^{-3} . N_2O_5 uptake would contribute to the
 173 NO_3 loss rate of 0.4 s^{-1} , which is much higher than the direct NO_3 loss through the
 174 reaction of NO_3 with VOCs. Therefore, N_2O_5 uptake was proposed to be dominantly

175 responsible for the NO₃ loss and the initial s(t) was set to 1. Eq. 3 can describe the
 176 sum concentration of NO₃ and N₂O₅. Assuming the equilibrium between NO₃ and
 177 N₂O₅ is maintained after a certain period, based on the temperature-dependent
 178 equilibrium rate constant (k_{eq}) and the modeled NO₂ at a certain time, Eq. 4 can be
 179 used to determine the ratio of N₂O₅ to NO₃. Combined, Eqs. 1–4 allow for the
 180 calculation of NO₃ and N₂O₅ concentrations considering stable NO₃ and N₂O₅ loss
 181 rate constants (k_{NO_3} and $k_{N_2O_5}$, respectively). In the second step, a new s(t) was
 182 calculated using the data from the first step (Eq. 5), new initial NO₂ and O₃
 183 concentrations were then approximated, and NO₃ and N₂O₅ values were derived using
 184 the same method as used in the first step. This process was repeated until the
 185 difference between the two s(t) values was less than 0.005. The number of
 186 adjustments to a new s(t) could not be calculated more than 10 times. Otherwise, the
 187 calculating process would become non-convergent.

188 The modeled N₂O₅ concentrations and given $k_{N_2O_5}$ were then used to estimate
 189 pNO₃⁻ formation. The HNO₃ produced in R4 was not considered because many of the
 190 products are organic nitrates (Brown and Stutz, 2012). Here, k_{NO_3} and $k_{N_2O_5}$ denote
 191 the pseudo-first-order reaction rate constants of the total NO₃ reactivity caused by
 192 ambient VOCs and N₂O₅ heterogeneous uptake, respectively. $k_{N_2O_5}$ is given in Eq. 6.
 193 S_a is the aerosol surface area, C is the mean molecular speed of N₂O₅, and $\gamma_{N_2O_5}$ is the
 194 N₂O₅ uptake coefficient. Sunset and sunrise times during the measurements were
 195 16:55 and 07:30 (Chinese National Standard Time, CNST), and the running time of
 196 the model set to 14.5 h from sunset to sunrise.

$$197 \quad \frac{d[O_3]}{dt} = -k_{NO_2+O_3}[O_3][NO_2] \quad (1)$$

$$198 \quad \frac{d[NO_2]}{dt} = -(1 + s(t)) \times k_{NO_2+O_3}[O_3][NO_2] \quad (2)$$

$$199 \quad \frac{d[NO_3+N_2O_5]}{dt} = k_{NO_2+O_3}[O_3][NO_2] - k_{N_2O_5}[N_2O_5] - k_{NO_3}[NO_3] \quad (3)$$

$$200 \quad \frac{[N_2O_5]}{[NO_3]} = k_{eq}[NO_2] \quad (4)$$

$$s(t) = \frac{\int_0^t k_{N_2O_5} \cdot [N_2O_5] dt + [N_2O_5]t}{[O_3](0) - [O_3](t)} \quad (5)$$

$$k_{N_2O_5} = \frac{C \times S_a \times \gamma_{N_2O_5}}{4} \quad (6)$$

203 Dry-state S_a at the PKU site was calculated based on the PNSD measurement,
 204 which was corrected to ambient (wet) S_a for particle hygroscopicity via a growth
 205 factor (Liu et al., 2013). The uncertainty of the wet S_a was estimated to be ~30%,
 206 which was associated with the error from dry PNSD measurement (~20%) and the
 207 growth factor (~20%). Nighttime averaged S_a on the night of December 19 was about
 208 $3000 \mu m^2 cm^{-3}$. PM measurements at the National Monitoring Sites proved this heavy
 209 haze pollution episode was a typical regional event (Fig. S1). Furthermore,
 210 synchronous study on the night of December 19, 2016, showed small variation in the
 211 vertical particle number concentration, with a boundary layer height of 340 m (Zhong
 212 et al., 2017). Overall, the S_a measured at the PKU site can represent the urban Beijing
 213 conditions in horizontal and vertical scale (< 340 m). Although the PNSD information
 214 for particles larger than $0.7 \mu m$ was not valid during the study period, the particles
 215 smaller than $0.7 \mu m$ dominated more than 95% of the aerosol surface area in a
 216 subsequent pollution episode (01/01/2017 to 01/07/2017), and similar results also
 217 were reported in other studies (e.g., Crowley et al., 2010a; Wang et al., 2018). The
 218 possible lower bias of S_a (5%) only led to a small overestimation of N_2O_5 , i.e.,
 219 3.6%–4.2%, and an underestimation of pNO_3^- of 0.2%–2.5% when $\gamma_{N_2O_5}$ varied from
 220 1×10^{-3} to 0.05.

221 The N_2O_5 uptake coefficient and $ClNO_2$ yield are key parameters in the estimation
 222 of pNO_3^- formation (Thornton et al., 2010; Riedel et al., 2013; Wagner et al., 2013;
 223 Phillips et al., 2016). Wagner et al. (2013) shows the significant pNO_3^- suppression of
 224 N_2O_5 uptake aloft in the wintertime in Denver, CO, USA, the uptake coefficient is
 225 0.005 when the percentage of pNO_3^- in the $PM_{2.5}$ mass concentration is 40%. As the
 226 proportion of nitrate in the particle mass concentration is similarly high in North
 227 China during wintertime (Sun et al., 2013, 2015a; Chen et al., 2015; Zheng et al.,
 228 2015; Wen et al., 2015), herein we fixed the uptake coefficient to 0.005 for the base
 229 model initial input. Because the model input of $ClNO_2$ yield only affects the value of

230 produced pNO_3^- concentration and would not change the modeled N_2O_5 concentration,
231 we set the initial f_{CINO_2} to zero. Previous work showed the averaged k_{NO_3} was 0.01 -
232 0.02 s^{-1} in summer Beijing, with BVOCs contributing significantly (Wang H et al.,
233 2017a; Wang et al., 2018). The intensity of BVOCs emissions decreased in wintertime,
234 owing to the lower temperature and weak solar radiation, thus the k_{NO_3} should be
235 smaller than it is in summer. In this work, the model input k_{NO_3} was set to an arbitrary
236 and relatively high value of 0.02 s^{-1} (equivalent to 0.2 ppbv isoprene + 40 parts per
237 trillion volume (pptv) monoterpene + 1.0 ppbv cis-2-butene), to constrain the impact
238 of N_2O_5 uptake in the model. A series of sensitivity tests was conducted to study the
239 uncertainties of the model simulation, and the detailed test sets are listed in Table 1,
240 included the test of N_2O_5 uptake coefficient and k_{NO_3} . The $\gamma_{\text{N}_2\text{O}_5}$ sensitivity tests were
241 set from 0.001 to 0.05, and the k_{NO_3} tests were set to 0.001 s^{-1} , 0.01 s^{-1} , and 0.1 s^{-1} .

242 In the calculation of the particulate nitration formation by N_2O_5 uptake, an
243 assumption is that all soluble nitrate formed from N_2O_5 uptake goes to the particle
244 phase rather than the gas phase. The assumption would lead to an upper bias as the
245 degassing of gas phase HNO_3 from particulate nitrate. While in winter Beijing, the
246 mixing ratio of NH_3 was rich to tens of ppbv and always much higher than the
247 nocturnal gas phase HNO_3 (e.g., Liu et al., 2017). The high NH_3 suppressed the
248 degassing of particulate nitrate effectively. The measurement of gas phase HNO_3 and
249 pNO_3^- in the surface layer of Beijing showed the soluble nitrate favor to particle phase
250 in winter, especially in polluted days. For example, the nocturnal ratio of pNO_3^- to
251 total soluble nitrate was larger than 0.95 on average (Liu et al., 2017). Due to the low
252 temperature and high RH at high altitude, the ratio would increase and the degassing
253 of particulate nitrate is negligible.

254

255 **3. Results and discussion**

256 **3.1 Ground-based observations.**

257 A severe winter PM pollution event lasted from December 16 to 22, 2016, in Beijing.
258 Figure 2a shows the time series of $\text{PM}_{2.5}$ and other relevant parameters based on

259 ground measurements at the PKU site. The mass concentration of PM_{2.5} began to
260 increase from December 16, reaching 480 $\mu\text{g m}^{-3}$ on December 20. A fast PM growth
261 event was captured, with an overall increment of 100 $\mu\text{g m}^{-3}$ on the night of December
262 19 (Fig. 2a). Throughout the pollution episode, the meteorological conditions
263 included high RH ($50\% \pm 16\%$) and low temperature (2 ± 3 °C). The slow surface
264 wind speed ($< 3 \text{ m s}^{-1}$) implied the atmosphere was stable (Fig. 2c, d). The daytime O₃
265 concentration was low, owing to high NO emission and weak solar radiation. After
266 sunset, O₃ at surface layer was rapidly titrated to zero by the elevated NO. The
267 presence of high NO concentrations would have strongly suppressed the concentration
268 of NO₃, further suppressing N₂O₅ near the ground. Figure 2b depicts the high amounts
269 of NO and NO₂ that were observed at ground level during the PM pollution episode,
270 suggesting that pNO₃⁻ production via N₂O₅ uptake was not important near the ground
271 during the winter haze episode.

272

273 **3.2 Tower observations.**

274 Six vertical measurements of the total oxidants ($\text{O}_x = \text{O}_3 + \text{NO}_2$) below 50 m were
275 consistent with those measured at ground level and are shown in Fig. S2, confirming
276 that the two sites are comparable. On the night of December 20 (Fig. 3a), the NO₂ and
277 NO from 0 – 240 m were abundant and conservative around 21:00, with
278 concentrations of 80 ppbv and 100 ppbv, respectively. The O₃ concentrations
279 remained zero during the nighttime (Fig. 3b). The vertical profile on December 20
280 suggests that at least below 240 m, the N₂O₅ chemistry was not important, which is
281 consistent with the results at ground level as mentioned above. The vertical profile on
282 December 19 was different with that on December 20. Figure 4a shows the vertical
283 profiles around 21:00 on December 19; NO was abundant from the ground to 100 m,
284 then gradually decreased to zero from 100 m to 150 m, and remained at zero above
285 150 m. The observed NO₂ concentration was 85 ± 2 ppbv below 100 m, which
286 gradually decreased from 100 m to 150 m, and was 50 ± 2 ppbv from 150 m to 240 m.
287 The observed O₃ concentrations below 150 m were below the instrumental limit of

288 detection (Fig. 4b). Above 150 m, the O₃ concentration was 20 ± 2 ppbv,
289 corresponding to zero NO concentration. With respect to O_x, the mixing ratio of O_x
290 was 85 ± 2 ppbv at lower altitudes, whereas the O_x concentration at higher altitudes
291 was 15 ppbv lower than that at lower altitudes (Fig. 4b). The O_x missing from the
292 higher altitude air mass indicated an additional nocturnal removal of O_x aloft.

293 Figure 5 depicts the vertical profiles of NO_x, O₃, and O_x at 09:30 on the morning of
294 December 20, which have similar features to those observed at 21:00 on December 19.
295 The vertical profiles suggested stratification still existed at that time. The amount of
296 O_x missing aloft in the morning increased to 25 ppbv at 240 – 260 m, demonstrating
297 that an additional 25 ppbv of O_x was removed or converted to other compounds at
298 higher altitudes than at the surface layer during the night from December 19 to 20.
299 Figure S3 shows the vertical profiles of NO, NO₂, O₃, and O_x at ~12:00 on December
300 18, when solar radiation was strong enough to mix the trace gases well in the vertical
301 direction. NO_x and O₃ were found to be well mixed indeed, with small variation from
302 the ground level to 260 m.

303

304 **3.3 Particulate nitrate formation aloft.**

305 N₂O₅ uptake is one of the two most important pathways of ambient NO_x loss and
306 pNO₃⁻ formation (Wagner et al., 2013; Stutz et al., 2010; Tsai et al., 2014). At high
307 altitudes (e.g., > 150 m), NO₃ and N₂O₅ chemistry can be initiated in the co-presence
308 of high NO₂ and significant O₃ levels. Therefore, N₂O₅ uptake could represent a
309 plausible explanation for the O_x observed missing at high altitude on the night of
310 December 19. To explore this phenomenon, a time-step box model was used to
311 simulate the NO₃ and N₂O₅ chemistry based on the observed vertical profiles of NO₂
312 and O₃ on the night of December 19.

313 In the base case, the average initial NO₂ and O₃ levels above 150 m at sunset were
314 61 ± 3 ppbv and 27 ± 6 ppbv, respectively. The measured NO₂ concentration at the
315 PKU site at sunset (local time, 16:55) was 61 ppbv and showed good consistency with
316 the model result. The modeled N₂O₅ concentration was zero below 150 m, as the high

317 level of NO made for rapidly consumption of the formed NO₃. In contrast, the
 318 modeled N₂O₅ concentrations at 21:00 above 150 m were in the range of 400–600
 319 pptv (Fig. 6a). The pNO₃⁻ formation by N₂O₅ heterogeneous uptake from sunset to the
 320 measurement time can be calculated using Eq. 7, which was significant of 24 μg m⁻³
 321 after sunset above 150 m. The pNO₃⁻ formed in 4.5 hours was equivalent to 13 ppbv
 322 O_x loss and consistent with the observation (15 ppbv) (Fig. 6b). Where the 1.5:1
 323 relationship between O_x and pNO₃⁻ was used to calculate the O_x equivalence (S. S.
 324 Brown et al., 2006).

$$325 \quad \sum p\text{NO}_3^- = \int_0^t (2 - f) \cdot k_{\text{N}_2\text{O}_5} \cdot [\text{N}_2\text{O}_5] dt \quad (7)$$

326 The box model enabled the analysis of the integrated pNO₃⁻ and ClNO₂ via N₂O₅
 327 uptake throughout the night. As shown in Fig. 6c, the modeled integrated pNO₃⁻ went
 328 as high as 50 μg m⁻³. The integrated pNO₃⁻ at sunrise was equal to the loss of 27 ppbv
 329 O_x, showing a good agreement with the observed O_x missing (25 ppbv) aloft in the
 330 morning hours. During the nighttime, the pNO₃⁻ formed aloft via N₂O₅ uptake led to
 331 the much higher particle nitrate concentration than that in the surface layer, which has
 332 been reported in many field observations (Watson et al., 2002; S. G. Brown et al.,
 333 2006; Lurmann et al., 2006; Ferrero et al., 2012; Sun et al., 2015b). The elevated
 334 pNO₃⁻ aloft was well dispersed through vertical mixing and enhanced the
 335 surface-layer PM concentration; this phenomenon was also observed in previous
 336 studies (Watson et al., 2002; S. G. Brown et al., 2006; Lurmann et al., 2006;
 337 Prabhakar et al., 2017). Zhong et al. (2017) showed that the NBL and PBL both were
 338 at 340 m from December 19 to 20, 2016 in Beijing. Daytime vertical downward
 339 transportation was helpful in mixing the air mass within the PBL. Assuming the newly
 340 formed pNO₃⁻ aloft from 150 m to 340 m is 50 μg m⁻³ during the nighttime and well
 341 mixed within the PBL in the next morning, the pNO₃⁻ enhancement at the surface
 342 layer (ΔpNO₃⁻) can be simplified to the calculation in Eq. 8 as following:

$$343 \quad \Delta p\text{NO}_3 = \frac{\int_0^{150} P(p\text{NO}_3) dH + \int_{150}^{340} P(p\text{NO}_3) dH}{340} \quad (8)$$

344 Here, $P(p\text{NO}_3^-)$ is the integral production of pNO₃⁻ and H represents height. Owing

345 to high NO below 150 m, the pNO₃⁻ formation via N₂O₅ uptake was zero. The
346 enhancement of pNO₃⁻ from 150 m to 340 m was calculated as 28 μg m⁻³, which is in
347 good agreement with the observed PM peak in the morning on December 20, with PM
348 enhancement of ~60 μg m⁻³. The result demonstrated that the nocturnal N₂O₅ uptake
349 aloft and downward transportation were critical for understanding the PM growth
350 process.

351

352 3.4 Sensitivity studies.

353 Previous studies have emphasized that the N₂O₅ uptake coefficient varies greatly
354 (0.001 – 0.1) in different ambient conditions (Chang et al., 2011; Brown and Stutz,
355 2012; Wang H et al., 2016), which is the main source of uncertainties in this model. In
356 the present research, sensitivity studies showed the modeled N₂O₅ concentration
357 dropping from 3 ppbv to 60 pptv when the N₂O₅ uptake coefficients increased from
358 0.001 to 0.05 (Fig. 6a), as the N₂O₅ concentration is very sensitive to the loss from
359 heterogeneous reactions. Compared to the base case, the accumulated pNO₃⁻ was
360 evidently lower at γ = 0.001 (44 μg m⁻³). Low N₂O₅ uptake coefficients correspond to
361 several types of aerosols, such as secondary organic aerosols (Gross et al., 2009),
362 humic acids (Badger et al., 2006), and certain solid aerosols (Gross et al., 2008).
363 When the N₂O₅ uptake coefficient increased from 0.005 to 0.05 (Fig. 6b, c), the
364 increase in integral pNO₃⁻ was negligible. The conversion capacity of N₂O₅ uptake to
365 pNO₃⁻ is maximized for a given, fixed value of the ClNO₂ yield. The conversion of
366 NO_x to pNO₃⁻ was not limited by the N₂O₅ heterogeneous reaction rate, but limited by
367 the formation of NO₃ via the reaction of NO₂ with O₃ during the polluted night.

368 For describing the nocturnal NO_x removal capacity and pNO₃⁻ formation via NO₃
369 and N₂O₅ chemistry, the overnight NO_x loss efficiency (ε) was calculated using Eq. 9.

$$370 \quad \varepsilon = \frac{\int_0^t 2 \times k_{\text{N}_2\text{O}_5} [\text{N}_2\text{O}_5] dt + \int_0^t k_{\text{NO}_3} [\text{NO}_3] dt}{[\text{NO}_2](0)} \quad (9)$$

371 The case modeled typical winter haze pollution conditions in Beijing from sunset to
372 sunrise, with the initial model values of NO₂ and O₃ set to 60 ppbv and 30 ppbv,

373 respectively. S_a was set to $3000 \mu\text{m}^2 \text{cm}^{-3}$, the ClNO_2 yield was zero, and k_{NO_3} was
374 0.02 s^{-1} . The reaction time was set to 14.5 h to represent an overnight period in
375 wintertime. The consumed NO_3 by the reaction with VOCs and N_2O_5 by uptake
376 reaction were regarded as NO_x removal. Figure 7 shows the dependence of the
377 overnight NO_x loss efficiency on the N_2O_5 uptake coefficient, as it varied from 1×10^{-5}
378 to 0.1. This is an increase from 20% to 56% with increasing $\gamma_{\text{N}_2\text{O}_5}$, which is similar to
379 the result addressed by Chang et al. (2011). The ceiling of overnight NO_x loss via
380 NO_3 - N_2O_5 chemistry was fixed when all the NO_x loss was through N_2O_5 uptake in
381 polluted days, which is limited by the reaction time and the formation rate of NO_3
382 (R1). In this case, the N_2O_5 uptake contributed about 90% of the overnight NO_x loss
383 (50.4%) when $\gamma_{\text{N}_2\text{O}_5}$ was equal to 2×10^{-3} . When $\gamma_{\text{N}_2\text{O}_5}$ was less than 2×10^{-3} , NO_x
384 removal increased rapidly with the increasing of $\gamma_{\text{N}_2\text{O}_5}$, which was defined as the
385 $\gamma_{\text{N}_2\text{O}_5}$ -sensitive region. When $\gamma_{\text{N}_2\text{O}_5} \geq 2 \times 10^{-3}$, the contribution of N_2O_5 uptake to NO_x
386 loss was over 90% and became insensitive. This region was defined as the
387 $\gamma_{\text{N}_2\text{O}_5}$ -insensitive region. According to Eqs. 3 and 5, high S_a , high NO_x , low k_{NO_3} or
388 low temperature allow the N_2O_5 uptake more easily located in the $\gamma_{\text{N}_2\text{O}_5}$ -insensitive
389 region. Here, the critical value of the N_2O_5 uptake coefficient (2×10^{-3}) was relatively
390 low compared with that recommended for the surface of mineral dust (0.013,
391 290-300K) (Crowley et al., 2010b; Tang et al., 2017) or determined in many field
392 experiments (e.g., S. S. Brown et al., 2006; 2009; Wagner et al., 2013; Morgan et al.,
393 2015; Phillips et al., 2016; Wang Z et al., 2017; Brown et al., 2016; Wang H et al.,
394 2017b; Wang X et al., 2017). This suggests that the NO_x loss and pNO_3^- formation by
395 N_2O_5 uptake were easily maximized in the pollution episode, and further worsening
396 the PM pollution.

397 In the base case, the modeled pNO_3^- formation via N_2O_5 uptake was an upper limit
398 result, as the ClNO_2 yield was set to zero. High coal combustion emitted chloride into
399 the atmosphere of Beijing during the heating period (Sun et al., 2013), like the
400 emissions from power plants in north China. This enhanced anthropogenic chloride
401 provides abundant chloride-containing aerosols to form ClNO_2 via N_2O_5 uptake aloft,
402 implying that significant ClNO_2 formed in the upper layer of the NBL (Tham et al.,

403 2016; Wang Z et al., 2017). Assuming the ClNO₂ yield is the average value of 0.28
404 determined at high altitude in north China (Wang Z et al., 2017), the pNO₃⁻ produced
405 throughout the night decreased 7 μg m⁻³. The modeled formation of ClNO₂ aloft
406 throughout the night was 2.5 ppbv, which is comparable with the observation in North
407 China (Tham et al., 2016; Wang Z et al., 2017; Wang X et al., 2017). Since the
408 modeled pNO₃⁻ formation is sensitive to the ClNO₂ yield, a higher yield would
409 increase the model uncertainty directly, hence probing the ClNO₂ yield is warranted in
410 future studies. As for NO₃ reactivity, Fig. 8 shows the sensitivity tests of the integral
411 pNO₃⁻ formation for the whole night at k_{NO_3} values = 0.001 s⁻¹, 0.01 s⁻¹, 0.02 s⁻¹, and
412 0.05 s⁻¹. The integral pNO₃⁻ formation decreased when k_{NO_3} varied from 0.001 s⁻¹ to
413 0.1 s⁻¹, but the variation ratio to the base case was within 5%. The result shows the
414 NO₃-N₂O₅ loss via NO₃ reaction with VOCs during the polluted wintertime was not
415 important, which may only lead to relatively small uncertainties in the integral pNO₃⁻
416 formation calculation. Nevertheless, if N₂O₅ uptake was extremely low (e.g., $\gamma_{\text{N}_2\text{O}_5} <$
417 10⁻⁴), the uncertainty of NO₃ oxidation would increase significantly.

418 The uncertainty caused by the physical changes of the air masses were analyzed
419 from two folds, one is the dilution and the other is the mixing and exchange of the air
420 mass. With respect to the impact of the dilution process, it would decrease the mixing
421 ratio of NO₂, O₃, NO₃ and N₂O₅, and leads to a lower contribution to the particulate
422 nitrate formation. An additional loss process for trace gases with a lifetime of 24 h
423 was assumed for calculated species in the sensitivity test (Lu et al., 2012). The result
424 shows that the integrated production of particulate nitrate decreased 28% compared
425 with base case. With respect to the exchange and mixing of the air mass at high
426 altitude during nighttime in polluted winter, the stable atmospheric stratification was
427 featured with strong inversion (Zhong et al., 2017). The nocturnal atmosphere is
428 stable and layered, the upward mixing from the surface is minimized, and air masses
429 above the surface are less affected by nocturnal emissions (Wagner et al., 2013).
430 Nevertheless, the injection by warm combustion sources or the clean air mass can
431 affect the air mass in fact. If the warm combustion source emitted NO_x into the air
432 mass after sunset, which would increase the mixing ratio of O_x, and restart the zero

433 time of the model. Accounting for the uncertainties from the mixing, sensitivities tests
434 of the box model to shorting the duration of 25%, the bias of the integrated pNO_3^-
435 throughout the night was small within 12% relative to base case. If the air mass was
436 affected by the clean air mass from the north, it would be featured with very low NO_x
437 and about 40 ppbv O_3 (background condition), which was not consistent with our
438 observation.

439

440 **4. Conclusion**

441 During the wintertime, ambient O_3 is often fully titrated at the ground level in urban
442 Beijing owing to its fast reaction with NO emissions. Consequently, the near-surface
443 air masses are chemically inert. Nevertheless, the chemical information of the air
444 masses at higher altitudes was indicative of a reactive layer above urban Beijing,
445 which potentially drives fast pNO_3^- production via N_2O_5 uptake and contributes to the
446 surface PM mass concentration. In this study, we found a case to show evidence for
447 additional O_x missing (25 ppbv) aloft throughout the night. Based on model
448 simulation, we found that the particulate nitrate formed above 150 m reached $50 \mu\text{g}$
449 m^{-3} and enhanced the surface level PM concentration significantly by $28 \mu\text{g m}^{-3}$ with
450 downward mixing after break-up of the NBL in the morning.

451 Our result emphasized the importance of the heterogeneous chemistry aloft the city
452 through a case study. The model simulation also demonstrated that during the heavy
453 PM pollution period, the particulate nitrate formation capacity via N_2O_5 uptake was
454 easily maximized in the high altitude above urban Beijing, even with low N_2O_5 uptake
455 coefficient. This indicates that the mixing ratio of NO_2 aloft was directly linked to
456 nitrate formation, and reduction of NO_x is helpful in decreasing nocturnal nitrate
457 formation. Overall, this study highlights the importance of the interplay between
458 chemical formation aloft and dynamic processes for probing the ground-level PM
459 pollution problem. In the future, direct observations of N_2O_5 and associated
460 parameters should be performed to explore the physical and chemical properties of
461 this overhead nighttime reaction layer and to reach a better understanding of the

462 winter haze formation.

463

464

465 ***Acknowledgements.***

466 This work was supported by the National Natural Science Foundation of China (Grant
467 No. 91544225, 41375124, 21522701, 41571130021), the National Key Technology
468 Research and Development Program of the Ministry of Science and Technology of
469 China (Grant No. 2014BAC21B01). The authors gratefully acknowledge the science
470 team of Peking University for their general support, as well as the team running the
471 tower platform, which enabled the vertical profile observations.

472

473 **References.**

- 474 Baasandorj, M., Hoch, S. W., Bares, R., Lin, J. C., Brown, S. S., Millet, D. B., Martin, R., Kelly,
475 K., Zarzana, K. J., Whiteman, C. D., Dube, W. P., Tonnesen, G., Jaramillo, I. C., and Sohl, J.:
476 Coupling between Chemical and Meteorological Processes under Persistent Cold-Air Pool
477 Conditions: Evolution of Wintertime PM_{2.5} Pollution Events and N₂O₅ Observations in Utah's
478 Salt Lake Valley, *Environ Sci Technol*, 51, 5941-5950, 2017.
- 479 Badger, C. L., Griffiths, P. T., George, I., Abbatt, J. P. D., and Cox, R. A.: Reactive uptake of N₂O₅
480 by aerosol particles containing mixtures of humic acid and ammonium sulfate, *J Phys Chem*
481 *A*, 110, 6986-6994, 2006.
- 482 Benton, A. K., Langridge, J. M., Ball, S. M., Bloss, W. J., Dall'Osto, M., Nemitz, E., Harrison, R.
483 M., and Jones, R. L.: Night-time chemistry above London: measurements of NO₃ and N₂O₅
484 from the BT Tower, *Atmos Chem Phys*, 10, 9781-9795, 2010.
- 485 Bertram, T. H., Thornton, J. A., and Riedel, T. P.: An experimental technique for the direct
486 measurement of N₂O₅ reactivity on ambient particles, *Atmos Meas Tech*, 2, 231-242, 2009.
- 487 Birks, J. W., Andersen, P. C., Williford, C. J., Turnipseed, A. A., Strunk, S. E., Ennis, C. A., and
488 Mattson, E.: Folded Tubular Photometer for atmospheric measurements of NO₂ and NO,
489 *Atmos. Meas. Tech. Discuss.*, <https://doi.org/10.5194/amt-2018-24>, in review, 2018.
- 490 Brown, S. G., Roberts, P. T., McCarthy, M. C., Lurmann, F. W., and Hyslop, N. P.: Wintertime
491 vertical variations in particulate matter (PM) and precursor concentrations in the San Joaquin
492 Valley during the California Regional coarse PM/fine PM Air Quality Study, *J Air Waste*
493 *Manage*, 56, 1267-1277, 2006.
- 494 Brown, S. S., Neuman, J. A., Ryerson, T. B., Trainer, M., Dube, W. P., Holloway, J. S., Warneke,
495 C., de Gouw, J. A., Donnelly, S. G., Atlas, E., Matthew, B., Middlebrook, A. M., Peltier, R.,
496 Weber, R. J., Stohl, A., Meagher, J. F., Fehsenfeld, F. C., and Ravishankara, A. R.: Nocturnal
497 odd-oxygen budget and its implications for ozone loss in the lower troposphere, *Geophys Res*
498 *Lett*, 33, Artn L08801. 10.1029/2006gl025900, 2006.
- 499 Brown, S. S., Dube, W. P., Fuchs, H., Ryerson, T. B., Wollny, A. G., Brock, C. A., Bahreini, R.,

500 Middlebrook, A. M., Neuman, J. A., Atlas, E., Roberts, J. M., Osthoff, H. D., Trainer, M.,
501 Fehsenfeld, F. C., and Ravishankara, A. R.: Reactive uptake coefficients for N₂O₅ determined
502 from aircraft measurements during the Second Texas Air Quality Study: Comparison to
503 current model parameterizations, *J Geophys Res-Atmos*, 114, 2009.

504 Brown, S. S., Dube, W. P., Osthoff, H. D., Wolfe, D. E., Angevine, W. M., and Ravishankara, A. R.:
505 High resolution vertical distributions of NO₃ and N₂O₅ through the nocturnal boundary layer,
506 *Atmos Chem Phys*, 7, 139-149, 2007.

507 Brown, S. S., Dube, W. P., Tham, Y. J., Zha, Q. Z., Xue, L. K., Poon, S., Wang, Z., Blake, D. R.,
508 Tsui, W., Parrish, D. D., and Wang, T.: Nighttime chemistry at a high altitude site above Hong
509 Kong, *J Geophys Res-Atmos*, 121, 2457-2475, 2016.

510 Brown, S. S., Ryerson, T. B., Wollny, A. G., Brock, C. A., Peltier, R., Sullivan, A. P., Weber, R. J.,
511 Dube, W. P., Trainer, M., Meagher, J. F., Fehsenfeld, F. C., and Ravishankara, A. R.:
512 Variability in nocturnal nitrogen oxide processing and its role in regional air quality, *Science*,
513 311, 67-70, 2006.

514 Brown, S. S. and Stutz, J.: Nighttime radical observations and chemistry, *Chem Soc Rev*, 41,
515 6405-6447, 2012.

516 Cao, J. J., Xu, H. M., Xu, Q., Chen, B. H., and Kan, H. D.: Fine Particulate Matter Constituents
517 and Cardiopulmonary Mortality in a Heavily Polluted Chinese City, *Environ Health Persp*,
518 120, 373-378, 2012.

519 Chan, C. Y., Xu, X. D., Li, Y. S., Wong, K. H., Ding, G. A., Chan, L. Y., and Cheng, X. H.:
520 Characteristics of vertical profiles and sources of PM_{2.5}, PM₁₀ and carbonaceous species in
521 Beijing, *Atmos Environ*, 39, 5113-5124, 2005.

522 Chang, W. L., Bhave, P. V., Brown, S. S., Riemer, N., Stutz, J., and Dabdub, D.: Heterogeneous
523 Atmospheric Chemistry, Ambient Measurements, and Model Calculations of N₂O₅: A
524 Review, *Aerosol Sci Tech*, 45, 665-695, 10.1080/02786826.2010.551672, 2011.

525 Chang, W. L., Brown, S. S., Stutz, J., Middlebrook, A. M., Bahreini, R., Wagner, N. L., Dube, W.
526 P., Pollack, I. B., Ryerson, T. B., and Riemer, N.: Evaluating N₂O₅ heterogeneous hydrolysis
527 parameterizations for CalNex 2010, *J Geophys Res-Atmos*, 121, 5051-5070,
528 10.1002/2015jd024737, 2016.

529 Chen, C., Sun, Y. L., Xu, W. Q., Du, W., Zhou, L. B., Han, T. T., Wang, Q. Q., Fu, P. Q., Wang, Z.
530 F., Gao, Z. Q., Zhang, Q., and Worsnop, D. R.: Characteristics and sources of submicron
531 aerosols above the urban canopy (260 m) in Beijing, China, during the 2014 APEC summit,
532 *Atmos Chem Phys*, 15, 12879-12895, 2015.

533 Crowley, J. N., Ammann, M., Cox, R. A., Hynes, R. G., Jenkin, M. E., Mellouki, A., Rossi, M. J.,
534 Troe, J., and Wallington, T. J.: Evaluated kinetic and photochemical data for atmospheric
535 chemistry: Volume V - heterogeneous reactions on solid substrates, *Atmos Chem Phys*, 10,
536 9059-9223, 2010b.

537 Crowley, J. N., Schuster, G., Pouvesle, N., Parchatka, U., Fischer, H., Bonn, B., Bingemer, H., and
538 Lelieveld, J.: Nocturnal nitrogen oxides at a rural mountain-site in south-western Germany,
539 *Atmos Chem Phys*, 10, 2795-2812, 2010a.

540 Ferrero, L., Cappelletti, D., Moroni, B., Sangiorgi, G., Perrone, M. G., Crocchianti, S., and
541 Bolzacchini, E.: Wintertime aerosol dynamics and chemical composition across the mixing
542 layer over basin valleys, *Atmos Environ*, 56, 143-153, 2012.

543 Ferrero, L., Perrone, M. G., Petraccone, S., Sangiorgi, G., Ferrini, B. S., Lo Porto, C., Lazzati, Z.,

544 Cocchi, D., Bruno, F., Greco, F., Riccio, A., and Bolzacchini, E.: Vertically-resolved particle
545 size distribution within and above the mixing layer over the Milan metropolitan area, *Atmos*
546 *Chem Phys*, 10, 3915-3932, 2010.

547 Geyer, A., and Stutz, J.: Vertical profiles of NO₃, N₂O₅, O₃, and NO_x in the nocturnal boundary
548 layer: 2. Model studies on the altitude dependence of composition and chemistry, *J Geophys*
549 *Res-Atmos*, 109, Artn D12307 Doi 10.1029/2003jd004211, 2004.

550 Green, M. C.; Chow, J. C.; Watson, J. G.; Dick, K.; Inouye, D., Effects of snow cover and
551 atmospheric stability on winter PM_{2.5} concentrations in Western U.S. valleys. *J. Appl.*
552 *Meteor. Climatol.* 2015, 54 (6), 1191-1201. DOI 10.1175/JAMC-D-14-0191.1.

553 Gross, S. and Bertram, A. K.: Reactive uptake of NO₃, N₂O₅, NO₂, HNO₃, and O₃ on three types
554 of polycyclic aromatic hydrocarbon surfaces, *J Phys Chem A*, 112, 3104-3113, 2008.

555 Gross, S., Iannone, R., Xiao, S., and Bertram, A. K.: Reactive uptake studies of NO₃ and N₂O₅ on
556 alkenoic acid, alkanolate, and polyalcohol substrates to probe nighttime aerosol chemistry,
557 *Phys Chem Chem Phys*, 11, 7792-7803, 2009.

558 Grzanic, G., Bartels-Rausch, T., Berkemeier, T., Turler, A., and Ammann, M.: Viscosity controls
559 humidity dependence of N₂O₅ uptake to citric acid aerosol, *Atmos Chem Phys*, 15,
560 13615-13625, 2015.

561 Guo, S., Hu, M., Zamora, M. L., Peng, J. F., Shang, D. J., Zheng, J., Du, Z. F., Wu, Z., Shao, M.,
562 Zeng, L. M., Molina, M. J., and Zhang, R. Y.: Elucidating severe urban haze formation in
563 China, *P Natl Acad Sci USA*, 111, 17373-17378, 2014.

564 Hallquist, M., Stewart, D. J., Stephenson, S. K., and Cox, R. A.: Hydrolysis of N₂O₅ on
565 sub-micron sulfate aerosols, *Phys Chem Chem Phys*, 5, 3453-3463, 2003.

566 Huang, R. J., Zhang, Y. L., Bozzetti, C., Ho, K. F., Cao, J. J., Han, Y. M., Daellenbach, K. R.,
567 Slowik, J. G., Platt, S. M., Canonaco, F., Zotter, P., Wolf, R., Pieber, S. M., Bruns, E. A.,
568 Crippa, M., Ciarelli, G., Piazzalunga, A., Schwikowski, M., Abbaszade, G., Schnelle-Kreis, J.,
569 Zimmermann, R., An, Z. S., Szidat, S., Baltensperger, U., El Haddad, I., and Prevot, A. S. H.:
570 High secondary aerosol contribution to particulate pollution during haze events in China,
571 *Nature*, 514, 218-222, 2014.

572 Kane, S. M., Caloz, F., and Leu, M. T.: Heterogeneous uptake of gaseous N₂O₅ by (NH₄)₂SO₄,
573 NH₄H₂SO₄, and H₂SO₄ aerosols, *J Phys Chem A*, 105, 6465-6470, 2001.

574 Kim, Y. J., Spak, S. N., Carmichael, G. R., Riemer, N., and Stanier, C. O.: Modeled aerosol nitrate
575 formation pathways during wintertime in the Great Lakes region of North America, *J*
576 *Geophys Res-Atmos*, 119, 12420-12445, 2014.

577 Lei, H. and Wuebbles, D. J.: Chemical competition in nitrate and sulfate formations and its effect
578 on air quality, *Atmos Environ*, 80, 472-477, 2013.

579 Liu, M. X., Song, Y., Zhou, T., Xu, Z. Y., Yan, C. Q., Zheng, M., Wu, Z. J., Hu, M., Wu, Y. S., and
580 Zhu, T.: Fine particle pH during severe haze episodes in northern China, *Geophys Res Lett*,
581 44, 5213-5221, 10.1002/2017gl073210, 2017.

582 Lurmann, F. W., Brown, S. G., McCarthy, M. C., and Roberts, P. T.: Processes influencing
583 secondary aerosol formation in the San Joaquin Valley during winter, *J Air Waste Manage*, 56,
584 1679-1693, 2006.

585 Mentel, T. F., Sohn, M., and Wahner, A.: Nitrate effect in the heterogeneous hydrolysis of
586 dinitrogen pentoxide on aqueous aerosols, *Phys Chem Chem Phys*, 1, 5451-5457, 1999.

587 Morgan, W. T., Ouyang, B., Allan, J. D., Aruffo, E., Di Carlo, P., Kennedy, O. J., Lowe, D., Flynn,

588 M. J., Rosenberg, P. D., Williams, P. I., Jones, R., McFiggans, G. B., and Coe, H.: Influence
589 of aerosol chemical composition on N₂O₅ uptake: airborne regional measurements in
590 northwestern Europe, *Atmos Chem Phys*, 15, 973-990, 2015.

591 Pathak, R. K., Wang, T., and Wu, W. S.: Nighttime enhancement of PM_{2.5} nitrate in ammonia-poor
592 atmospheric conditions in Beijing and Shanghai: Plausible contributions of heterogeneous
593 hydrolysis of N₂O₅ and HNO₃ partitioning, *Atmos Environ*, 45, 1183-1191, 2011.

594 Pathak, R. K., Wu, W. S., and Wang, T.: Summertime PM_{2.5} ionic species in four major cities of
595 China: nitrate formation in an ammonia-deficient atmosphere, *Atmos Chem Phys*, 9,
596 1711-1722, 2009.

597 Phillips, G. J., Thieser, J., Tang, M. J., Sobanski, N., Schuster, G., Fachinger, J., Drewnick, F.,
598 Borrmann, S., Bingemer, H., Lelieveld, J., and Crowley, J. N.: Estimating N₂O₅ uptake
599 coefficients using ambient measurements of NO₃, N₂O₅, ClNO₂ and particle-phase nitrate,
600 *Atmos Chem Phys*, 16, 13231-13249, 2016.

601 Prabhakar, G., Parworth, C. L., Zhang, X. L., Kim, H., Young, D. E., Beyersdorf, A. J., Ziemba, L.
602 D., Nowak, J. B., Bertram, T. H., Faloon, I. C., Zhang, Q., and Cappa, C. D.: Observational
603 assessment of the role of nocturnal residual-layer chemistry in determining daytime surface
604 particulate nitrate concentrations, *Atmos Chem Phys*, 17, 14747-14770,
605 10.5194/acp-17-14747-2017, 2017.

606 Pusede, S. E., Duffey, K. C., Shusterman, A. A., Saleh, A., Laughner, J. L., Wooldridge, P. J.,
607 Zhang, Q., Parworth, C. L., Kim, H., Capps, S. L., Valin, L. C., Cappa, C. D., Fried, A.,
608 Walega, J., Nowak, J. B., Weinheimer, A. J., Hoff, R. M., Berkoff, T. A., Beyersdorf, A. J.,
609 Olson, J., Crawford, J. H., and Cohen, R. C.: On the effectiveness of nitrogen oxide
610 reductions as a control over ammonium nitrate aerosol, *Atmos Chem Phys*, 16, 2575-2596,
611 2016.

612 Riedel, T. P., Wagner, N. L., Dube, W. P., Middlebrook, A. M., Young, C. J., Ozturk, F., Bahreini,
613 R., VandenBoer, T. C., Wolfe, D. E., Williams, E. J., Roberts, J. M., Brown, S. S., and
614 Thornton, J. A.: Chlorine activation within urban or power plant plumes: Vertically resolved
615 ClNO₂ and Cl₂ measurements from a tall tower in a polluted continental setting, *J Geophys*
616 *Res-Atmos*, 118, 8702-8715, 2013.

617 Sander, S. P., et al. (2011), *Chemical Kinetics and Photochemical Data for Use in Atmospheric*
618 *Studies Evaluation Number 17*, JPL Publication 10-6 Rep., NASA Jet Propul. Lab, Pasadena,
619 California.

620 Seinfeld, J. H., Pandis, S.N., (2006). *Atmospheric Chemistry and Physics: from Air Pollution to*
621 *Climate Change (Second edition)*, John Wiley & Sons, Inc., Hoboken, New Jersey.

622 Stutz, J., Alicke, B., Ackermann, R., Geyer, A., White, A., and Williams, E.: Vertical profiles of
623 NO₃, N₂O₅, O₃, and NO_x in the nocturnal boundary layer: 1. Observations during the
624 Texas Air Quality Study 2000, *J Geophys Res-Atmos*, 109, Artn D12306
625 10.1029/2003jd004209, 2004.

626 Stutz, J., Wong, K. W., Lawrence, L., Ziemba, L., Flynn, J. H., Rappengluck, B., and Lefer, B.:
627 Nocturnal NO₃ radical chemistry in Houston, TX, *Atmos Environ*, 44, 4099-4106, 2010.

628 Su, X., Tie, X. X., Li, G. H., Cao, J. J., Huang, R. J., Feng, T., Long, X., and Xu, R. G.: Effect of
629 hydrolysis of N₂O₅ on nitrate and ammonium formation in Beijing China: WRF-Chem model
630 simulation, *Sci Total Environ*, 579, 221-229, 2017.

631 Sun, Y. L., Du, W., Wan, Q. Q., Zhang, Q., Chen, C., Chen, Y., Chen, Z. Y., Fu, P. Q., Wang, Z. F.,

632 Gao, Z. Q., and Worsnop, D. R.: Real-Time Characterization of Aerosol Particle Composition
633 above the Urban Canopy in Beijing: Insights into the Interactions between the Atmospheric
634 Boundary Layer and Aerosol Chemistry, *Environ Sci Technol*, 49, 11340-11347, 2015b.

635 Sun, Y. L., Wang, Z. F., Du, W., Zhang, Q., Wang, Q. Q., Fu, P. Q., Pan, X. L., Li, J., Jayne, J., and
636 Worsnop, D. R.: Long-term real-time measurements of aerosol particle composition in
637 Beijing, China: seasonal variations, meteorological effects, and source analysis, *Atmos Chem
638 Phys*, 15, 10149-10165, 2015a.

639 Sun, Y. L., Wang, Z. F., Fu, P. Q., Yang, T., Jiang, Q., Dong, H. B., Li, J., and Jia, J. J.: Aerosol
640 composition, sources and processes during wintertime in Beijing, China, *Atmos Chem Phys*,
641 13, 4577-4592, 2013.

642 Tang, M. J., Thieser, J., Schuster, G., and Crowley, J. N.: Kinetics and Mechanism of the
643 Heterogeneous Reaction of N₂O₅ with Mineral Dust Particles, *Phys. Chem. Chem. Phys.*, 14,
644 8551-8561, 2012.

645 Tang, M. J., Huang, X., Lu, K. D., Ge, M. F., Li, Y. J., Cheng, P., Zhu, T., Ding, A. J., Zhang, Y. H.,
646 Gligorovski, S., Song, W., Ding, X., Bi, X. H., and Wang, X. M.: Heterogeneous reactions of
647 mineral dust aerosol: implications for tropospheric oxidation capacity, *Atmos. Chem. Phys.*,
648 17, 11727-11777, 2017.

649 Tham, Y. J., Wang, Z., Li, Q. Y., Yun, H., Wang, W. H., Wang, X. F., Xue, L. K., Lu, K. D., Ma, N.,
650 Bohn, B., Li, X., Kecorius, S., Gross, J., Shao, M., Wiedensohler, A., Zhang, Y. H., and Wang,
651 T.: Significant concentrations of nitryl chloride sustained in the morning: investigations of
652 the causes and impacts on ozone production in a polluted region of northern China, *Atmos
653 Chem Phys*, 16, 14959-14977, 2016.

654 Thornton, J. A., Braban, C. F., and Abbatt, J. P. D.: N₂O₅ hydrolysis on sub-micron organic
655 aerosols: the effect of relative humidity, particle phase, and particle size, *Phys Chem Chem
656 Phys*, 5, 4593-4603, 2003.

657 Thornton, J. A., Kercher, J. P., Riedel, T. P., Wagner, N. L., Cozic, J., Holloway, J. S., Dube, W. P.,
658 Wolfe, G. M., Quinn, P. K., Middlebrook, A. M., Alexander, B., and Brown, S. S.: A large
659 atomic chlorine source inferred from mid-continental reactive nitrogen chemistry, *Nature*,
660 464, 271-274, 2010.

661 Tsai, C., Wong, C., Hurlock, S., Pikelnaya, O., Mielke, L. H., Osthoff, H. D., Flynn, J. H., Haman,
662 C., Lefer, B., Gilman, J., de Gouw, J., and Stutz, J.: Nocturnal loss of NO_x during the 2010
663 CalNex-LA study in the Los Angeles Basin, *J Geophys Res-Atmos*, 119, 13004-13025, 2014.

664 Wagner, N. L., Riedel, T. P., Young, C. J., Bahreini, R., Brock, C. A., Dube, W. P., Kim, S.,
665 Middlebrook, A. M., Ozturk, F., Roberts, J. M., Russo, R., Sive, B., Swarthout, R., Thornton,
666 J. A., VandenBoer, T. C., Zhou, Y., and Brown, S. S.: N₂O₅ uptake coefficients and nocturnal
667 NO₂ removal rates determined from ambient wintertime measurements, *J Geophys
668 Res-Atmos*, 118, 9331-9350, 2013.

669 Wahner, A., Mentel, T. F., and Sohn, M.: Gas-phase reaction of N₂O₅ with water vapor:
670 Importance of heterogeneous hydrolysis of N₂O₅ and surface desorption of HNO₃ in a large
671 teflon chamber, *Geophys Res Lett*, 25, 2169-2172, 1998.

672 Wang, G. H., Zhang, R. Y., Gomez, M. E., Yang, L. X., Zamora, M. L., Hu, M., Lin, Y., Peng, J. F.,
673 Guo, S., Meng, J. J., Li, J. J., Cheng, C. L., Hu, T. F., Ren, Y. Q., Wang, Y. S., Gao, J., Cao, J.
674 J., An, Z. S., Zhou, W. J., Li, G. H., Wang, J. Y., Tian, P. F., Marrero-Ortiz, W., Secret, J., Du,
675 Z. F., Zheng, J., Shang, D. J., Zeng, L. M., Shao, M., Wang, W. G., Huang, Y., Wang, Y., Zhu,

676 Y. J., Li, Y. X., Hu, J. X., Pan, B., Cai, L., Cheng, Y. T., Ji, Y. M., Zhang, F., Rosenfeld, D.,
677 Liss, P. S., Duce, R. A., Kolb, C. E., and Molina, M. J.: Persistent sulfate formation from
678 London Fog to Chinese haze, *P Natl Acad Sci USA*, 113, 13630-13635,
679 10.1073/pnas.1616540113, 2016.

680 Wang, H. C. and Lu, K. D.: Determination and Parameterization of the Heterogeneous Uptake
681 Coefficient of Dinitrogen Pentoxide (N_2O_5), *Prog Chem*, 28, 917-933, 2016.

682 Wang, H. C., Lu, K. D., Chen, X. R., Zhu, Q. D., Chen, Q., Guo, S., Jiang, M. Q., Li, X., Shang, D.
683 J., Tan, Z. F., Wu, Y. S., Wu, Z. J., Zou, Q., Zheng, Y., Zeng, L. M., Zhu, T., Hu, M., and
684 Zhang, Y. H.: High N_2O_5 Concentrations Observed in Urban Beijing: Implications of a Large
685 Nitrate Formation Pathway, *Environ Sci Tech Lett*, 4, 416-420, 2017b.

686 Wang, H. C., Lu, K. D., Tan, Z. F., Sun, K., Li, X., Hu, M., Shao, M., Zeng, L. M., Zhu, T., and
687 Zhang, Y. H.: Model simulation of NO_3 , N_2O_5 and ClNO_2 at a rural site in Beijing during
688 CAREBeijing-2006, *Atmos Res*, 196, 97-107, 2017a.

689 Wang, H., Lu, K., Guo, S., Wu, Z., Shang, D., Tan, Z., Wang, Y., Le Breton, M., Zhu, W., Lou, S.,
690 Tang, M., Wu, Y., Zheng, J., Zeng, L., Hallquist, M., Hu, M., and Zhang, Y.: Efficient N_2O_5
691 Uptake and NO_3 Oxidation in the Outflow of Urban Beijing, *Atmos. Chem. Phys. Discuss.*,
692 <https://doi.org/10.5194/acp-2018-88>, in review, 2018.

693 Wang, X. F., Wang, H., Xue, L. K., Wang, T., Wang, L. W., Gu, R. R., Wang, W. H., Tham, Y. J.,
694 Wang, Z., Yang, L. X., Chen, J. M., and Wang, W. X.: Observations of N_2O_5 and ClNO_2 at a
695 polluted urban surface site in North China: High N_2O_5 uptake coefficients and low ClNO_2
696 product yields, *Atmos Environ*, 156, 125-134, 2017.

697 Wang, Z., Wang, W. H., Tham, Y. J., Li, Q. Y., Wang, H., Wen, L., Wang, X. F., and Wang, T.: Fast
698 heterogeneous N_2O_5 uptake and ClNO_2 production in power plant and industrial plumes
699 observed in the nocturnal residual layer over the North China Plain, *Atmos Chem Phys*, 17,
700 12361-12378, 2017.

701 Watson, J. G. and Chow, J. C.: A wintertime $\text{PM}_{2.5}$ episode at the fresno, CA, supersite, *Atmos*
702 *Environ*, 36, 465-475, 2002.

703 Wen, L. A., Chen, J. M., Yang, L. X., Wang, X. F., Xu, C. H., Sui, X. A., Yao, L., Zhu, Y. H.,
704 Zhang, J. M., Zhu, T., and Wang, W. X.: Enhanced formation of fine particulate nitrate at a
705 rural site on the North China Plain in summer: The important roles of ammonia and ozone,
706 *Atmos Environ*, 101, 294-302, 2015.

707 Ying, Q.: Physical and chemical processes of wintertime secondary nitrate aerosol formation,
708 *Front Environ Sci En*, 5, 348-361, 2011.

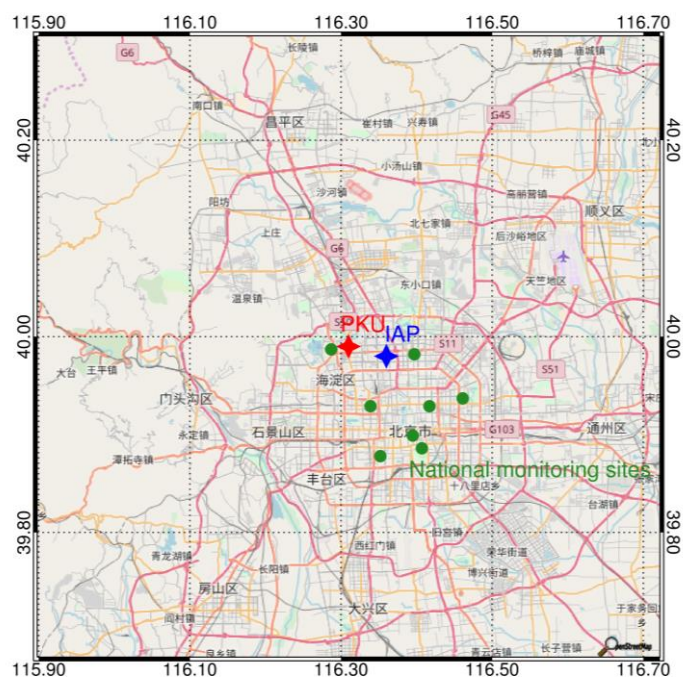
709 Zhang, Q., Jimenez, J. L., Canagaratna, M. R., Allan, J. D., Coe, H., Ulbrich, I., Alfarra, M. R.,
710 Takami, A., Middlebrook, A. M., Sun, Y. L., Dzepina, K., Dunlea, E., Docherty, K., DeCarlo,
711 P. F., Salcedo, D., Onasch, T., Jayne, J. T., Miyoshi, T., Shimojo, A., Hatakeyama, S.,
712 Takegawa, N., Kondo, Y., Schneider, J., Drewnick, F., Borrmann, S., Weimer, S., Demerjian,
713 K., Williams, P., Bower, K., Bahreini, R., Cottrell, L., Griffin, R. J., Rautiainen, J., Sun, J. Y.,
714 Zhang, Y. M., and Worsnop, D. R.: Ubiquity and dominance of oxygenated species in organic
715 aerosols in anthropogenically-influenced Northern Hemisphere midlatitudes, *Geophys Res*
716 *Lett*, 34, 2007.

717 Zhang, R. Y., Wang, G. H., Guo, S., Zarnora, M. L., Ying, Q., Lin, Y., Wang, W. G., Hu, M., and
718 Wang, Y.: Formation of Urban Fine Particulate Matter, *Chem Rev*, 115, 3803-3855, 2015.

719 Zheng, G. J., Duan, F. K., Su, H., Ma, Y. L., Cheng, Y., Zheng, B., Zhang, Q., Huang, T., Kimoto,

720 T., Chang, D., Poschl, U., Cheng, Y. F., and He, K. B.: Exploring the severe winter haze in
721 Beijing: the impact of synoptic weather, regional transport and heterogeneous reactions,
722 Atmos Chem Phys, 15, 2969-2983, 2015.

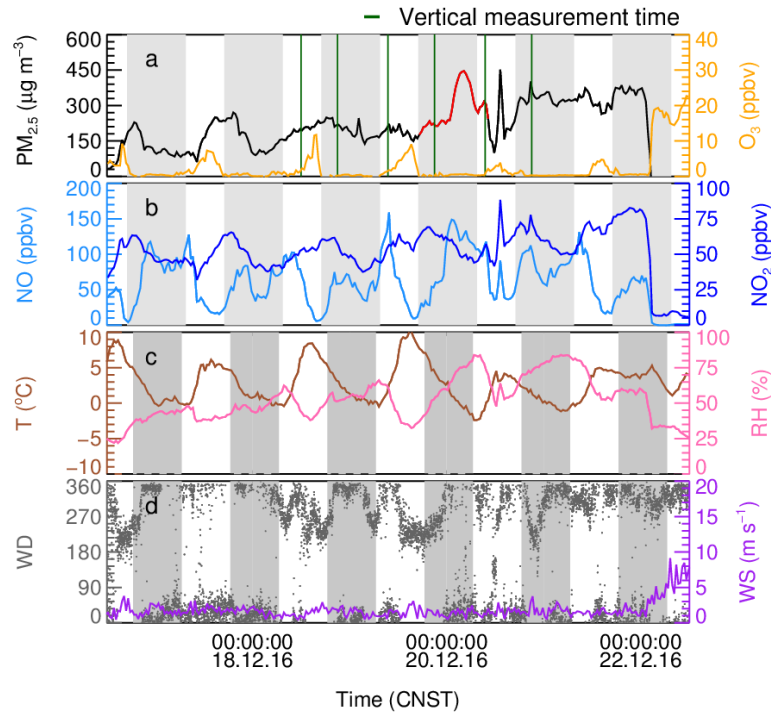
723 Zhong, J. T., Zhang, X. Y., Wang, Y. Q., Sun, J. Y., Zhang, Y. M., Wang, J. Z., Tan, K. Y., Shen,
724 X. J., Che, H. C., Zhang, L., Zhang, Z. X., Qi, X. F., Zhao, H. R., Ren, S. X., and Li, Y.:
725 Relative Contributions of Boundary-Layer Meteorological Factors to the Explosive Growth
726 of PM_{2.5} during the Red-Alert Heavy Pollution Episodes in Beijing in December 2016, J
727 Meteorol Res-Prc, 31, 809-819, 2017.



728

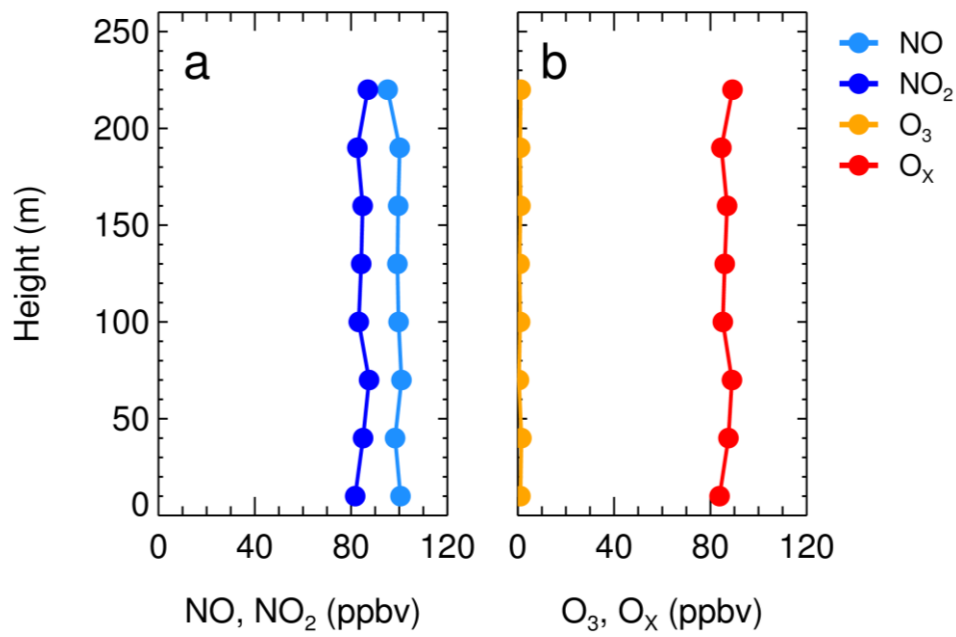
729 **Figure 1.** Location of the monitoring sites used in this study, including PKU (red
 730 diamond), IAP (blue diamond), and other National Monitoring Sites (green circles).
 731 Vertical profiles of NO_x and O_3 were collected at a tower at the IAP. Measurements of
 732 particle number and size distribution (used to calculate N_2O_5 and particle nitrate
 733 formation) were collected from a ground site at PKU. Additional measurements on
 734 $\text{PM}_{2.5}$ concentrations were continuously measured at national monitoring sites
 735 throughout Beijing.

736



737

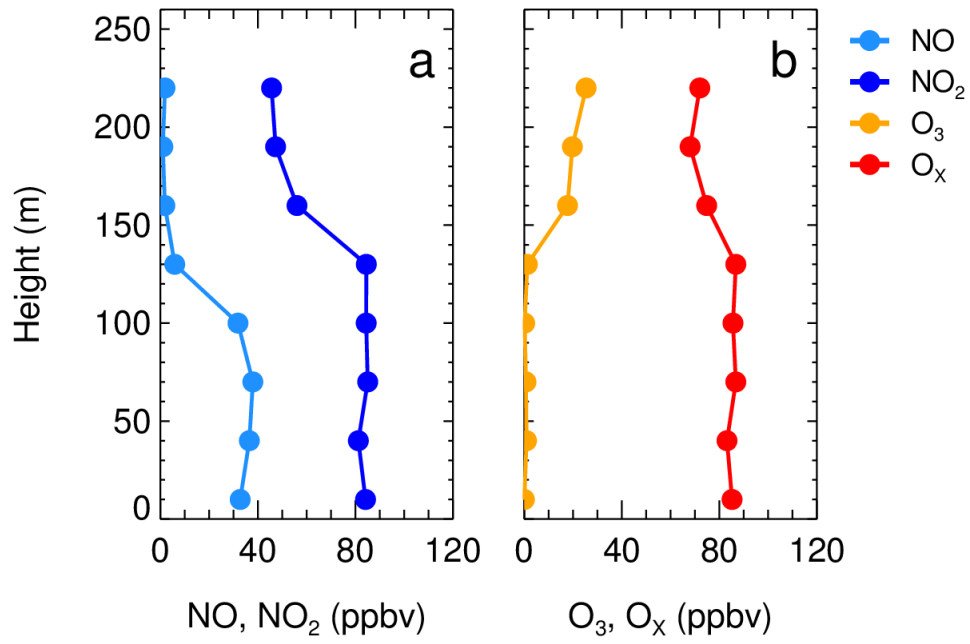
738 **Figure 2.** Time series of (a) $PM_{2.5}$ and O_3 , (b) NO and NO_2 , (c) temperature (T) and
 739 relative humidity (RH), (d) wind direction (WD) and wind speed (WS) from
 740 December 16 to 22, 2016 at PKU site in Beijing, China. The shaded region represents
 741 the nighttime periods. Red line in panel (a) shows an example of fast $PM_{2.5}$
 742 enhancement on the night of December 19, and the green lines are the time periods
 743 when the vertical measurements conducted in IAP site.



744

745 **Figure 3.** Vertical profiles of NO and NO₂ (a), O₃ and O_x (b) at 20:38-21:06 on the
 746 night of December 20, 2016.

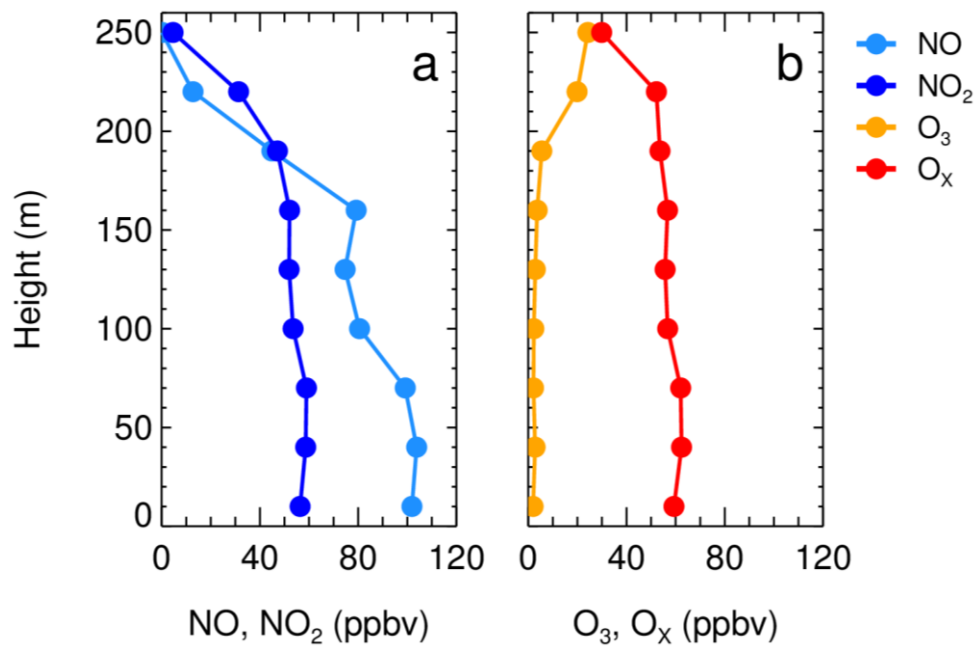
747



748

749 **Figure 4.** O_x missing case presented by the vertical profiles of (a) NO and NO₂, (b)
 750 O₃ and O_x at 20:38-21:13 on the night of December 19, 2016.

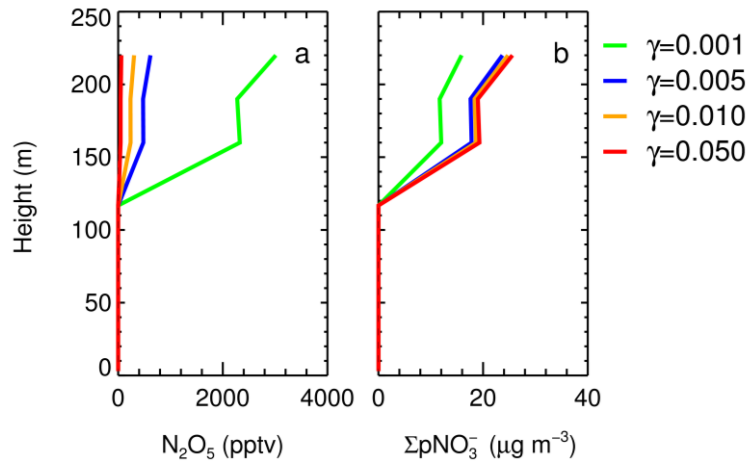
751



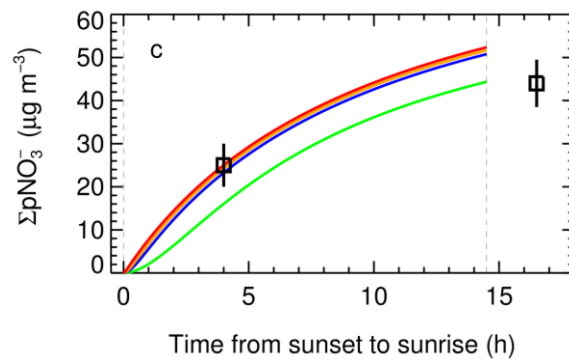
752

753 **Figure 5.** Vertical profiles of (a) NO and NO₂, (b) O₃ and O_x at 09:06-09:34 in the
 754 morning of December 20, 2016.

755



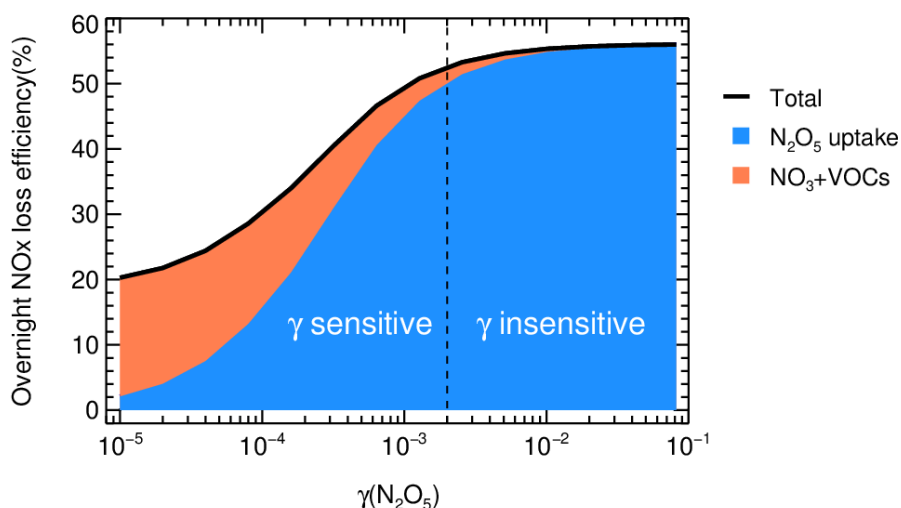
756



757

758 **Figure 6.** Base case ($\gamma=0.005$) and sensitivity tests of the vertical profile on the night
 759 of December 19 at different N_2O_5 uptake coefficients, including (a) the mixing ratio
 760 of N_2O_5 at 21:00, (b) the integral pNO_3^- production from sunset to 21:00, (c) the time
 761 series of the integral pNO_3^- formed at 240 m via N_2O_5 uptake from sunset (17:00) to
 762 sunrise (07:30, nighttime length = 14.5 h), the squares represents the pNO_3^- equivalent
 763 weight from the observed O_x missing in the two vertical measurements \sim 21:00 and
 764 \sim 09:30 in the following morning.

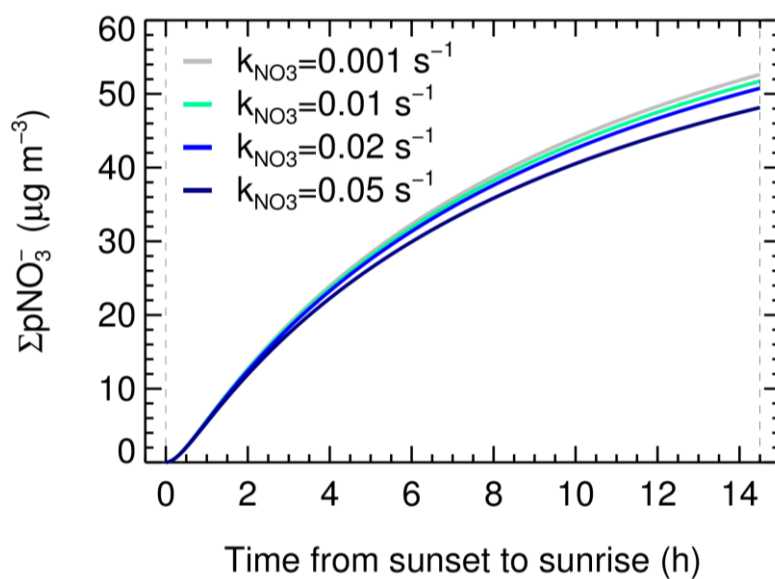
765



766

767 **Figure 7.** The dependence of overnight NO_x loss via N₂O₅ uptake on $\gamma_{\text{N}_2\text{O}_5}$ in a typical
 768 winter pollution condition. The initial NO₂ and O₃ were set to 60 ppbv and 30 ppbv,
 769 respectively, S_a was set to 3000 $\mu\text{m}^2 \text{cm}^{-3}$, the ClNO₂ yield was zero and k_{NO_3} was 0.02
 770 s^{-1} . The reaction time was set to 14.5 h. The blue and orange zone represent the
 771 contribution by NO₃+VOCs and N₂O₅ uptake, the dashed line ($\gamma = 0.002$, when N₂O₅
 772 uptake contribute to 90% of the maximum NO_x loss) divide the loss into γ sensitive
 773 and insensitive region. The maximum nocturnal NO_x loss by NO₃-N₂O₅ chemistry is
 774 56%.

775



776

777 **Figure 8.** Base case ($k_{\text{NO}_3}=0.02 \text{ s}^{-1}$) and sensitivity tests of the integral $p\text{NO}_3^-$ formed

778 at 240 m via N_2O_5 uptake at different NO_3 reactivity (0.001 s^{-1} , 0.01 s^{-1} , 0.05 s^{-1}) on

779 the whole night of December 19, 2016.

780

781

Table 1. List of the parameter sets in base case and sensitivity tests.

Cases	k_{NO_3} (s^{-1})	$\gamma_{\text{N}_2\text{O}_5}$
Base case	0.02	0.005
k_{NO_3} test 1	0.001	0.005
k_{NO_3} test 2	0.01	0.005
k_{NO_3} test 3	0.05	0.005
$\gamma_{\text{N}_2\text{O}_5}$ test 1	0.02	0.001
$\gamma_{\text{N}_2\text{O}_5}$ test 2	0.02	0.01
$\gamma_{\text{N}_2\text{O}_5}$ test 3	0.02	0.05

782